

# Original Research Article

## **Nondestructive and accurate detection of transparent liquid mass fraction based on Snell's law**

---

### **ABSTRACT**

Based on the Snell's law, one can convert the liquid mass fraction into the spot displacement by directing a laser into the trapezoidal component containing the solution. In this physical experiment, the trapezoidal component was designed to facilitate convenient replacement of liquids, and the CCD sensor was used to accurately record the spot position. The accurate results of liquid mass fraction was achieved by fitting sinusoidal-cubic functions after theoretical modification. In this study, the refractive index of the measured solution ranges from 1.333-1.414, with an actual resolution of approximately 0.0003. The mass fraction resolution accuracy is roughly  $\pm 0.2\%$  for sodium chloride, sucrose, and *D*-glucose while it is  $\pm 0.4\%$  for ethanol solution. This resolution has increased in comparison to similar physical principle experiments, and it can now successfully fulfill the daily detection criteria for the transparent liquid mass fraction.

*Keywords: Liquid mass fraction; Refractive index; Spot displacement; CCD*

### **1. INTRODUCTION**

Transparent liquid is very common in our daily life, the detection and control of its composition and content have a direct correlation with the quality and safety of products. For instance, changes in the composition of soda water, sugar juice, fruit drinks, and wine will have an impact on the safety and quality of the products [1]. At the same time, accurate measurement of liquid mass fraction is also needed in basic research, chemical analysis, pollutant detection, diagnostics, semiconductor manufacturing and other fields. Therefore, how to measure the mass fraction of transparent liquid simply, quickly and accurately is of great significance in scientific research and production practice.

Physically, the mass fraction of the transparent liquid can be acquired by measuring the physical quantities of the solution such as optical rotation [2-3], absorbance [4-5], capacitance [6], electrical conductivity [7], refractive index [8-10], etc. Refractive index is a frequently employed index. Under certain conditions, the mass fraction of liquid has a linear relationship with refractive index [11-12]. The law of refraction can be used to measure the refractive index in a variety of ways, including the mirage principle technique [8], complete reflection principle method [13], skimming incidence method [14], and CCD measurement method [15-16]. However, the tested solution is disposable for these measuring methods above, and the solution replacement is very inconvenient [8, 13-16]. In this experiment, the liquid can be easily nondestructively replaced through an electric pump and an inventively designed opened glass component. At the same time, this device has better accuracy with the high precision TCD1035DG CCD compared to the results in other literatures [15-16]. The CCD here is used to measure the mass fraction of the solution, and the refractive index is converted into the displacement of the light spot on CCD by the refraction law. The functional relationship between the mass fraction of different solutions and the offset is obtained by theoretical analysis and experimental fitting. Then the mass fraction of the solution can be obtained by measuring the offset and simply solving the function formula, and the experiment has a high precision. Different from previous experiments [15-16], the fitting curve in this experiment is nonlinear, the measurement findings are precise and trustworthy, and the approach is straightforward and useful.

According to Maxwell's electromagnetic field theory, the refractive index of solution  $n$  can be expressed as  $n = (\epsilon_r \mu_r)^{1/2}$ . The relative permeability of transparent liquid in the optical frequency band is in general  $\mu_r = 1$ . Therefore,  $n \approx \epsilon_r^{1/2}$  while the relative dielectric constant  $\epsilon_r$  is related to the polarization and temperature of the applied electric field. Hence,  $n$  is determined by the physical properties of the solution itself, namely the type and mass fraction. As a result, under a unified temperature environment with single laser wavelength, the mass fraction of the solution  $w$  of a certain type liquid can match to the refractive index  $n$  one by one, and satisfy the relationship of linear function [11-12, 17-18].

## 2. METHODOLOGY AND EXPERIMENTAL DETAILS

### 2.1 Experimental Apparatus

Experimental instruments: high collimation laser, trapezoidal quartz component, AT89S52 single-chip circuit board, TCD1035DG monochrome CCD sensor, oscilloscope, polarizer, beaker, glass rod, sucrose, sodium chloride, anhydrous ethanol, D-glucose, analytical balance, DC power supply, creep pump, ruler, leather tube.

### 2.2 Measurement Fundamentals

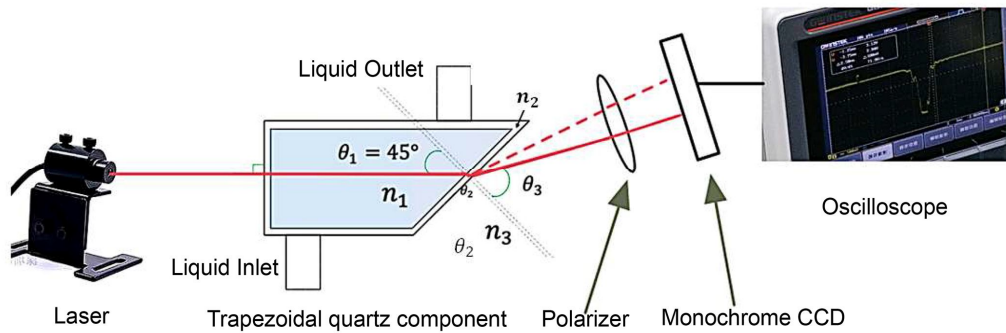


**Fig.1. Schematic diagram of the mass fraction measurement device.**

Figure 1 shows the schematic diagram of the liquid mass fraction measurement device. The refraction effect as indicated in Figure 1 will happen when the laser is directly incident into the trapezoidal quartz component holding transparent liquid. The acute angle of the trapezoidal component made of JGS-2 optical glass is  $45^\circ$ , and then the light will pass through the polarizer for attenuation and fall on the CCD sensor. Through the program on the self-designed circuit board, the CCD spot position can be converted into electrical signal input oscilloscope. Let the refractive index of solution be  $n_1$ , the refractive index of quartz glass  $n_2$  and the refractive index of air  $n_3 = 1$ . When the incident light in the outgoing region, according to the Snell's Law, it can be known that:

$$n_1 \sin(\pi/4) = n_2 \sin \theta_2 = \sin \theta_3 \quad (1)$$

As the mass fraction of the solution under test rises, that is,  $n_1$  increases, so does  $\theta_2$  and  $\theta_3$ . If  $n_2$  is greater than 1, the upper limit of angle  $\theta_3$  will reach  $\pi/2$  first, which  $n_1$  is upper bounded by 1.414. Considering that the refractive index of pure water at  $20^\circ\text{C}$  is 1.333, the measured solution  $n_1$  can be measured from 1.333 to 1.414. It is noted that with the  $n_1$  increasing, the position of the emerging laser spot at the glass-air interface will have a slight upward shift, which theoretically will further increase the displacement of the emerging light spot on the CCD, thus improving the resolution of the experiment. However, considering that the thickness of the component is only 3 mm, this micro deviation can be nearly ignored in the subsequent analysis.

### 2.3 Theoretical Accuracy Estimation

By differentiating both sides of formula (1), the formula of the change of the exit angle  $\theta_3$  with the refractive index  $n_1$  is obtained

$$dn_1 = 2^{1/2} \cos \theta_3 d\theta_3 \quad (2)$$

The variation of the outgoing light spot's movement  $\Delta s$  on CCD with the outgoing angle  $\Delta \theta_3$  can be simplified as  $ds = R d\theta_3$ , which can be obtained by using formula (1)

$$ds = R(2 - n_1^2)^{-1/2} dn_1 \quad (3)$$

In this device, the distance between the emerging light spot and the CCD is  $R = 50$  cm. As shown in formula (3), when the change rate of the refractive index  $\Delta n_1$  is fixed at 0.001, the offset of the light spot on the CCD  $\Delta s$  varies with the change of  $n_1$ , as shown in Figure 2 below.

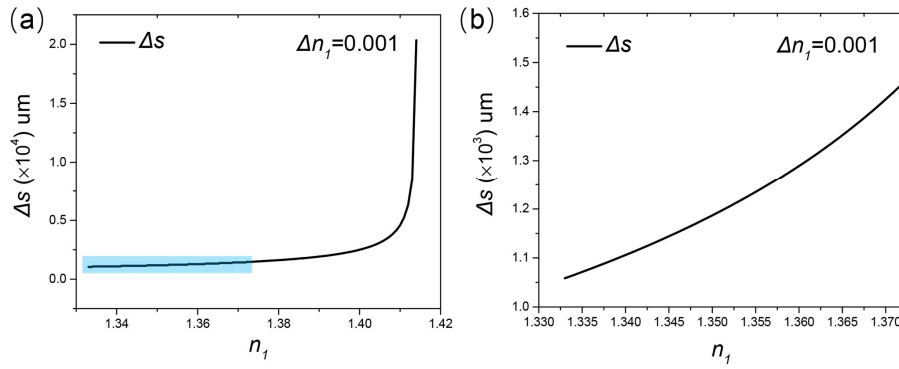


**Fig. 2. (a) The offset of the light spot on the CCD  $\Delta s$  changes with the refractive index of solution  $n_1$ . (b) the enlargement figure of the blue area in (a).**

It can be seen from Figure 2 that the offset of the light spot  $\Delta s$  on the CCD increases slowly with the rise  $n_1$  and increases rapidly when  $n_1$  approaches the measurable refractive index threshold of 1.414. Figure 2(b) is an enlarged view of the blue area in Figure 2(a). It can be seen from the Figure 2(b) that even in the region with very low mass fraction, when the refractive index change  $\Delta n_1$  is only 0.001, the light spot offset  $\Delta s$  reaches 1 mm from the leftmost part of the curve.

The CCD model used in this device is TCD1035DG, which has 3648 rows of pixels. The transverse size of a single pixel point is 8  $\mu\text{m}$  which means it can distinguish the change of light point  $\Delta s$  in the order of 8  $\mu\text{m}$ . By making a simple transformation of formula (3), when the light spot offset remains unchanged at 8  $\mu\text{m}$ , the change of refractive index  $\Delta n_1$  with  $n_1$  is shown in Figure 3 below.

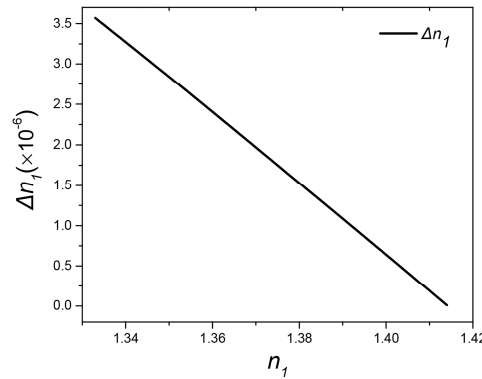


**Fig. 3. The change of refractive index of solution  $\Delta n_1$  versus  $n_1$ .**

From Figure 3, it can be concluded that  $\Delta n_1$  theoretically detected by CCD ranges from  $3.5 \times 10^{-6}$  below to  $1.0 \times 10^{-6}$ . The refractive index  $n_1$  resolution of theoretical solutions can be at least  $1.0 \times 10^{-5}$ .

## 2.4 Spot Displacement Analysis

Integral calculation was done on formula (3) in order to obtain the appropriate relationship between refractive index  $n_1$  and the displacement of the light spot  $S$  on CCD. When pure water is used, the position of light spot on CCD is the initial origin, then

$$\begin{aligned}
 S &= \int_0^s ds \\
 &= \int_{1.333}^{n_1} R(2 - n_1^2)^{-1/2} dn_1 \\
 &= R \sin^{-1}(2^{-1/2} n_1) - R \sin^{-1}(2^{-1/2} \times 1.333)
 \end{aligned}$$

Hence

$$n_1 = 2^{-1/2} \sin\left(\frac{S}{R} + \sin^{-1}\left(2^{-1/2} \times 1.333\right)\right) \quad (4)$$

Equation (4) above is a typical sinusoidal function, and Figure 4 was drawn as follows for intuitive understanding. It can be seen from the figure that the refractive index of solution  $n_1$  increases with  $S$  nonlinearity, and the accuracy is improved as  $n_1$  approaches the measured threshold of 1.414.

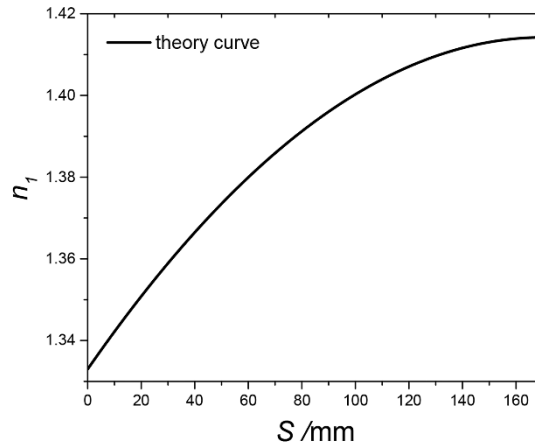


**Fig. 4. The relation between therefractive index  $n_1$  and the displacement  $S$  of light spot on CCD.**

Since the mass fraction of the solution  $w$  and the refractive index  $n_1$  satisfy the linear function [11-12, 17], the function relation  $w$  with the displacement  $S$  can be obtained by combining formula (4).

$$w = a \sin\left(\frac{S}{R} + \sin^{-1}\left(2^{-1/2} \times 1.333\right)\right) + b \quad (5)$$

Where  $a$  and  $b$  are unknown constants. Considering the simplification of the analysis derived from formula (2) to formula (3), and the inevitable micro-deviation of the position of the light spot at the glass-air interface with the  $n_1$  increasing, and further considering the Taylor expansion form of sine function, the fitting formula (5) is modified by adding a cubed small quantity  $cS^3$  to better fit the experimental data, where  $c$  is the unknown small constant. Therefore, the fitting function adopted is sinusoidal - cubic function.

$$w = a \sin\left(\frac{S}{R} + \sin^{-1}\left(2^{-1/2} \times 1.333\right)\right) + b + cS^3 \quad (6)$$

## 2.5 Experiment Preparation

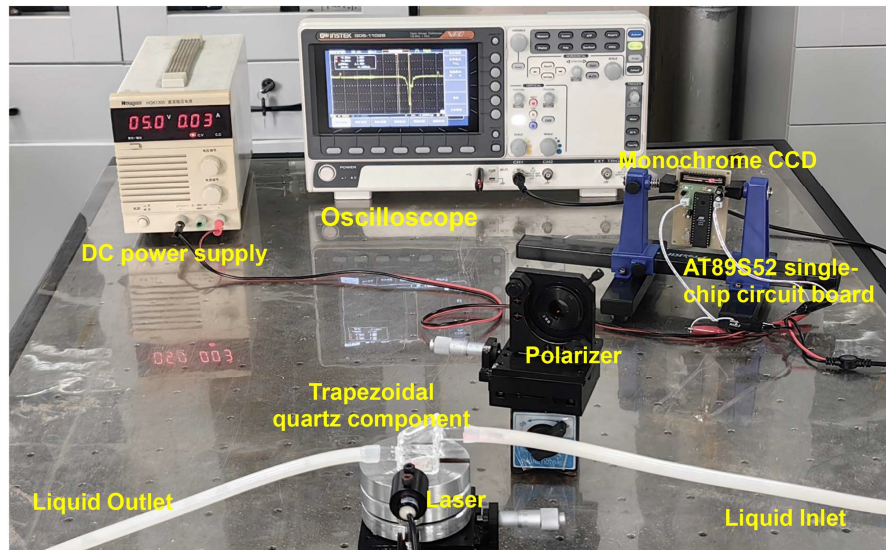


**Fig. 5. Liquid mass fraction measurement device.**

1) The liquid mass fraction detection device was constructed on the optical platform with high collimation laser, trapezoidal quartz glass component, polarizer, circuit board including CCD sensor, DC power supply and other equipment, as shown in Figure 5.

2) Sodium chloride (sucrose, *D*-glucose, anhydrous ethanol) was mixed with pure water, and four solutions ranging from 4% to 24% with an interval of 4% were prepared by using an electronic balance with an accuracy of 0.01g and an analytical balance with an accuracy of 0.0001g.

3) The solution was carefully placed in a 20°C-controlled laboratory environment. Since ethanol is volatile, the ethanol solution must be prepared on the spot.

## 2.6 Experimental Procedures

- 1) Adjust the laser to ensure the collimation of the **outgoing 655 ± 5nm light** and adjust the level of the trapezoid component so that the light is incident on the plane of the trapezoid component.
- 2) Open the pumping pump to adjust the pumping speed, extract pure water to the trapezoidal component for 2 minutes. Place the monochrome sensor perpendicular to the emerging light to ensure the distance  $R = 50$  cm, and then move the CCD so that the emerging light spot lands on the right side of the CCD. This **should be** done after optimizing the optical path.
- 3) Adjust the oscilloscope and polarizer, so that the light waveform can be completely displayed in the oscilloscope, and then adjust the trigger pulse time.
- 4) The change of environment and the instability of the system would inevitably lead to slight fluctuation of the position waveform of the light spot, so the pure water in the component is replaced three times to determine the stability of the device. The experimental test results showed that the fluctuation deviation error of the system is about 0.3 mm. According to formula (3), the actual resolution  $n_1$  of the system is about  $2.83 \times 10^{-4}$ .
- 5) Use the pump to extract the solution with different mass fractions  $w$  into the component successively, record the waveform positions of different solutions in the oscilloscope. Take the average data to reduce the system error by extracting the solution mass fractions and recording the positions for three times.
- 6) According to the formula analyzed above, the data fitting was carried out to obtain the formula between the mass fraction  $w$  of the four solutions and the displacement of the spot  $S$  on the CCD.

### 3. RESULTS AND DISCUSSION

The device was used to measure four kinds of solutions with mass **fractions  $w$  ranging** from 0% to 24%. Figure 6 shows the spot locations of four kinds of solutions with different mass fractions displayed on the oscilloscope during three tests. Due to the large offset of the light spot, it is necessary to move the position of the CCD, so the data of 12% and **20%** are recorded twice in each test for the superposition of the light spot position to ensure the accuracy of the data. The figure shows that the displacement of the light spot rises nonlinearly with increasing mass fraction, with ethanol solution growing least and sodium chloride solution increasing most. Table 1 displays the data from the four solutions that were taken from Figure 6 with the light spot position set to 0 mm **when  $w$  was 0%**. According to the theoretical analysis in Section 2.4 above, Formula (7) was fitted to the four groups of data in Table 1. The fitting curve results are shown in Figure 7. The solid points represented the means of the three measurements, and the solid lines represented the curves that fitted.

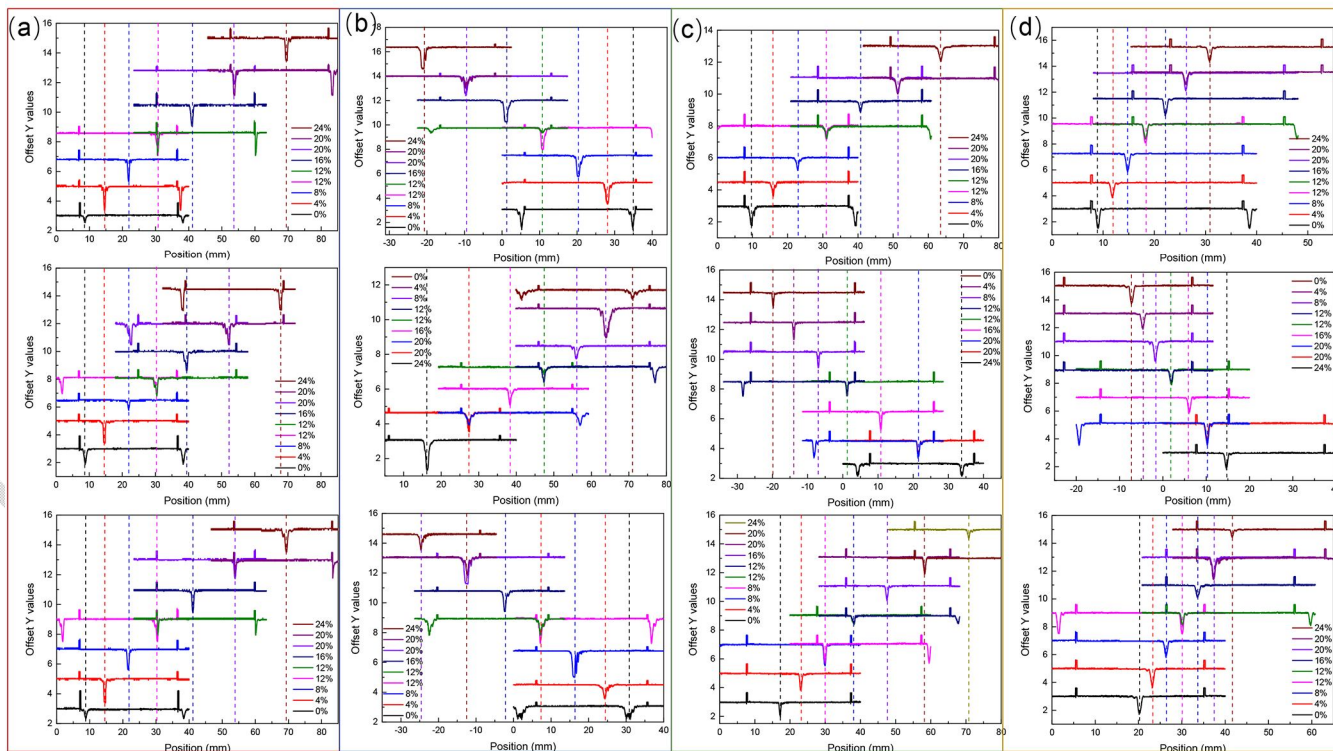


Fig. 6. Location diagram of the mass fraction of (a) sodium chloride, (b) sucrose, (c) *D*-glucose, and (d) ethanol solution under three measurements.

Table 1. Experimental measurement data of four solutions

$w\%$	Sodium Chloride		Sucrose		<i>D</i> -glucose		Ethanol	
	$S/\text{mm}$	$\bar{S}/\text{mm}$	$S/\text{mm}$	$\bar{S}/\text{mm}$	$S/\text{mm}$	$\bar{S}/\text{mm}$	$S/\text{mm}$	$\bar{S}/\text{mm}$
4	6.11		5.67		5.98		2.81	
	5.96	6.00	5.84	5.87	5.64	5.78	2.75	2.83
	5.92		6.11		5.73		2.92	
8	13.48		12.55		13.1		5.80	
	13.17	13.20	13.19	13.11	12.82	12.87	5.61	5.87
	12.96		13.59		12.70		6.18	
12	22.03		21.44		21.29		9.35	
	21.74	21.82	21.49	21.67	21.04	21.07	9.10	9.46
	21.7		22.08		20.88		9.92	
16	32.55		30.67		30.95		13.14	
	30.75	31.88	31.1	31.22	30.66	30.64	13.36	13.35
	32.35		31.89		30.30		13.54	
20	45.22		41.51		41.59		17.14	
	43.47	44.61	42.23	42.42	41.38	41.32	17.44	17.28
	45.13		43.52		40.98		17.24	
24	61.06		55.57		53.79		21.82	
	59.17	60.61	55.57	55.71	53.72	53.70	21.94	21.74
	60.69		55.99		53.56		21.46	

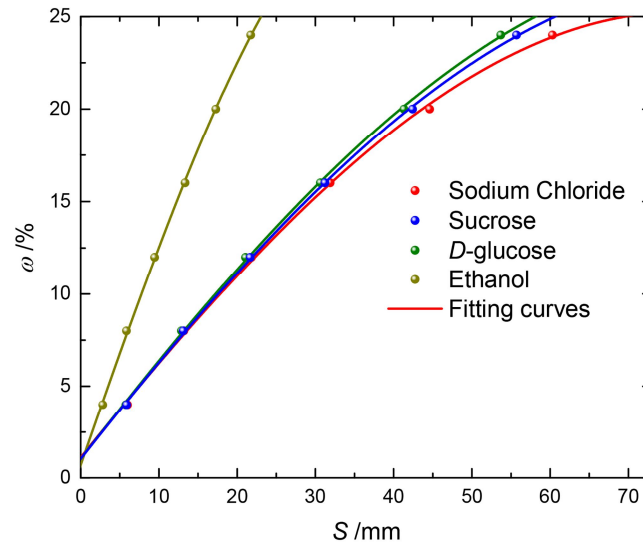


Fig.7. The relationship between the mass fraction  $w$  of four solutions and the displacement  $S$  of light spots.

It can be seen from the Figure 7 that all the four solutions can perform very good fitting, and the fitting curve line is highly consistent with the theoretical analysis shown in Figure 4. The p values of the fitting curves are all less than 0.001, indicating that the function model has high accuracy.

Formula group (7) gives the function fitting results of the four solutions:

$$\begin{cases}
 w_1 = 7.951 \times 10^2 \times \sin(S/500 + 1.230) - 7.483 \times 10^{-2} - 1.690 \times 10^{-5} \times S^3 \\
 w_2 = 8.113 \times 10^2 \times \sin(S/500 + 1.230) - 7.637 \times 10^{-2} - 1.430 \times 10^{-5} \times S^3 \\
 w_3 = 8.261 \times 10^2 \times \sin(S/500 + 1.230) - 7.776 \times 10^{-2} - 1.410 \times 10^{-5} \times S^3 \\
 w_4 = 1.853 \times 10^3 \times \sin(S/500 + 1.230) - 1.746 \times 10^{-3} - 1.920 \times 10^{-4} \times S^3
 \end{cases} \quad (7)$$

Where  $w_1$ ,  $w_2$ ,  $w_3$  and  $w_4$  represent the mass fraction of sodium chloride, sucrose, *D*-glucose and ethanol solutions respectively. Since the fluctuation error of the system itself is about 0.3mm, according to the formula group (7), the **mass**

fraction resolution accuracy of the system for sodium chloride, sucrose and *D*-glucose solution can reach  $\pm 0.2\%$ , and that of ethanol solution can reach  $\pm 0.4\%$ . At a uniform temperature, the derivative of the refractive index  $n$  with respect to the mass fraction  $w$  is different for different solutions [17-18]. The  $\partial n/\partial w$  of ethanol is much smaller than sodium chloride, sucrose, and *D*-glucose [17-18], which results in a much lower resolution accuracy of ethanol than the other three solutions.

In order to verify the accuracy of the experiment and the reliability of the fitting results, double-blind verification was carried out on the four solutions. The experimental test values of sodium chloride, sucrose, *D*-glucose, and ethanol solutions were 34.5mm, 22.3mm, 30.3mm and 23.8mm, respectively. Therefore, the mass fractions obtained by formula group (7) are 16.91%, 12.11%, 16.02% and 25.33%, respectively, and the actual mass fractions of the four solutions configured are 17%, 12%, 16% and 25%. It can be seen that the experiment has high accuracy and precision.

#### 4. CONCLUSION

In this physical experiment, the liquid can be simply changed through an electric pump and an opened glass component. The refraction light offset signal is then obtained based on the Snell's law and CCD, so as to realize the nondestructive detection of the mass fraction of transparent liquid. After four kinds of solution tests and double-blind verification, the experimental results can be fitted by the modified sinusoidal-cubic function, and the fitting results have high accuracy and precision. The device composed of this physical experiment can measure the refractive index of the solution within the range from 1.333 to 1.414, and the actual resolution is about 0.0003. For sodium chloride, sucrose and *D*-glucose, the mass fraction resolution accuracy is  $\pm 0.2\%$ , and for ethanol solution, the resolution accuracy is  $\pm 0.4\%$ , which is better than the previous test results of the same principle [15-16]. Because of its accessible application and straightforward operation, the device can be utilized for accurate nondestructive testing of transparent solutions in addition to being an exploratory experimental instrument for determining solution mass fraction. As for nonpolar solutes or solutes that form non-ideal solutions. Our method should be modified by designing the total reflection measurement element with a temperature controller. This would further improve the accuracy of the device while expanding the range of measurable solutions.

#### REFERENCES

1. Kregiel, D. Health Safety of Soft Drinks: Contents, Containers, and Microorganisms. *BioMed Research International*, 2015, 2015: 128697.
2. Li Dongyu, Huang Zhen, Li Chao, etc. Glucose Concentration Sensing Based on Orthogonal Reflection Multiple Polarization Rotation Effect. *Laser & Optoelectronics Progress*, 2022, 59 (21): 244-249. Chinese.
3. Li Guihua, Cong Xiaoyan, Zhang Hong, Zhao Wenli. The Teaching Research of Measuring the Concentration of Glucose Solution with Two Kinds of Polarimeter. *Physical Experiment of College*, 2021, 34 (02): 48-51. Chinese.
4. Yang Zebin, Hong Linger, Liu Zhaohui. Real Time Measurement of Solution Concentration Based on Double Beam Optical Path. *Physical Experiment of College*, 2022, 35 (05): 68-72. Chinese.
5. Zhu Ling, Zheng Hong, Wang Zhongping, etc. Measuring absorption spectra of Rodamine 6G solution using grating monochromator. *Physics Experimentation*, 2018, 38 (S1): 1-3. Chinese.
6. Du Quan, Zhang Ping, Liu Longjian. An Experimental Research on the Sensing Elements of Capacitance Liquid Concentration. *Physical Experiment of College*, 1999, 12 (02): 13-15. Chinese.
7. Chen Limei, Cheng Minxi, Xiao Xiaofang, etc. Measurement of the Relationship between Conductivity of Salt Solution and Concentration and Temperature. *Research And Exploration In Laboratory*, 2010, 29 (05): 39-42. Chinese.
8. Li Hanyi, Xiong Anguo, Wang Zheng, etc. Measuring the refractive index and chromatic dispersion of salt solution using hollow triple prism. *Physics Experimentation*, 2020, 40 (09): 51-54. Chinese.
9. Hu Kaiqi, Wang Huiqin, Lai Shengyong, Fan Weizheng. Household research on the relationship between mass fraction and refractive index of transparent liquid. *Physics Experimentation*, 2023, 43 (02): 49-53. Chinese.
10. Wei Wei, Peng Qiwei, Liu Caixia, Zhang Ting, Ruan Qianxiao. Measuring refractive index of solution based on mirage principle. *Physics Experimentation*, 2022, 42 (05): 30-34. Chinese.
11. Zhou Wanfu, Luo Shuangling, Wang Chuankun, Zhang Xing. The experience formula about the connector of the different liquid concentration and refractive index. *Journal of Minzu Normal University of Xingyi*, 2013 (05): 119-

- 121.Chinese.
12. Bai Zesheng, Liu Zhuqin, Xu Hong. An experienced formula about the connectic on of refraction index and consistence of several liquid.Journal of Yan'an University (Natural Science Edition), 2004,23 (01): 33-36.Chinese.
  13. JinZehua, Sun Liyuan, Zang Jianwen, etc. Designand manufactureof liquid refractiveindex measuring devicebasedontotalrefractionprinciple. Physics and Engineering, 2021,31 (03): 129-132.Chinese.
  14. Gold cleaning, KeJianhong. Measurement of Liquid's Index of Refraction and Concentration by a Method of Glancing incidence.Research and Exploration in Laboratory, 2002,21 (03): 52-57.Chinese.
  15. Guo Shanhe, Tian Yunxia, QiaoYali and so on. The study of measuring transparent liquid consistency in refraction process. Optical technology, 1996 (05): 36-37.Chinese.
  16. Chen Yi, Li Hong. Design of an emulsion concentration detection system based on the principle of total light reflection. Software Guide, 2016,15 (08): 130-133.Chinese.
  17. Chan-Yuan Tan, Yao-Xiong Huang, Dependence of Refractive Index on Concentration and Temperature in Electrolyte Solution, Polar Solution, Nonpolar Solution, and Protein Solution,J. Chem. Eng. Data, 2015, 60(10): 2827–2833.
  18. Haynes W M.CRC Handbook of Chemistry and Physics[M].Boca Raton:CRC Press,2012